

Microstructure, Texture and Residual Stresses of Hot-Extruded AlSi-Alloys

A.Pyzalla [1], J.Wegener [1], K.B.Müller [2] and K.-D.Liss [3]

[1] Strukturforschung, Hahn-Meitner-Institut, D - 14109 Berlin, Germany

[2] Forschungszentrum Strangpressen, TU-Berlin, D - 13355 Berlin, Germany

[3] ESRF Grenoble, BP220, F-38043 Grenoble, France

1 Abstract

The influence of the extrusion temperature on the microstructure, the texture and the residual stresses in the aluminum alloy AlSi25Cu4Mg1 after indirect extrusion is studied using microscopical methods as well as X-rays and high energy synchrotron X-rays.

2 Introduction

Hot extrusion processes are widely used for manufacturing semi-finished products and profiles, e.g. Al-profiles used in automobiles. Since the demands on components besides sufficient material strength often comprise high wear resistance interest has grown in extruded AlSi-composites with a high content of Si-particles. In order to enable a hot extrusion of these metal matrix composites new manufacturing routes have been developed /1, 2/. In the process used by /1/ first a billet is generated by spraying. The billet may be annealed and then is hot-extruded.

The aim of the experiments described here is the determination of the influence of the extrusion temperature on the microstructure, the texture and the residual stresses in AlSi25Cu4Mg1.

3 Extrusion process

The extrusion trials were carried out on the 8 MN horizontal extrusion press at the Extrusion Research and Development Center of Technical University of Berlin. For the measurement of axial forces the press employs load cells. By means of a computer aided measuring and evaluation system, die force, friction force and total extrusion force can be determined in

Table 1: Extrusion Parameters

Billet Diameter	Container Diameter	Die Diameter	Extrusion Ratio	$T_{\text{Billet}} = T_{\text{Container}} = T_{\text{Die}}$	Speed of Extrudates
105 mm	110 mm	35 mm	10:1	300°C / 400°C / 450°C	15 mm/s

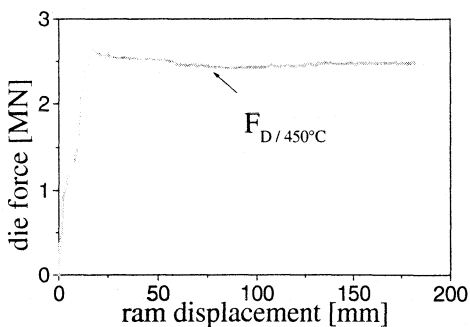


Figure 1 Die force versus ram displacement

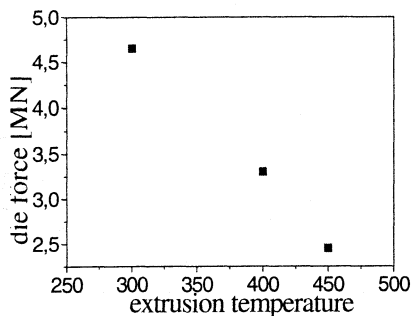


Figure 2: Die force vs. extrusion temperature

relation to the ram displacement [3]. The extrusion conditions are displayed in tab. 1. From former investigation with High-Silicon-Content Al-Alloys [4-6], high values of the hot deformation resistance for such kind of materials are known. In this case the high strength workability determined the choice of the extrusion method. Indirect extrusion of the above mentioned material was preferred. The important advantage of indirect extrusion is the absence of friction between the billet and the container. This guarantees a largely homogeneous flow of the material and an important decrease of the required total extrusion force. In indirect extrusion the billet is stationary and the die is pressed towards the billet. The force required thus due to lack of friction force is lower than in case of direct extrusion. Here, the die force was registered versus the ram displacement during the hot extrusion process for billets with initial temperatures varying between 450° C and 300° C. Higher extrusion temperatures lead to the formation of hot cracks. Obviously, the die force necessary decreases with increasing temperature of the billets (fig. 1, fig. 2), thus due to the force required, extrusion at lower temperatures than 350°C were not possible here.

4 Microstructure of the extrudates

The microstructure of the extrudates was studied by optical, scanning and transmission electron microscopy. The microstructure after extrusion shows a homogeneous distribution of about 25 vol.-% fine Si-particles in the aluminum matrix (fig. 3). The particle diameter varies between 5 μm and 15 μm , approximately. Optical microscopy reveals no differences in the microstructure of the samples extruded at 300° C and those extruded at the highest extrusion temperature 450° C considered here. The same holds for scanning electron and transmission electron micrographs. These techniques, however, both given evidence of twins in the Si-particles of all samples studied (fig. 4). Further investigations of the microstructure of the unextruded billet will be necessary in order to clarify the origin of the twinning.

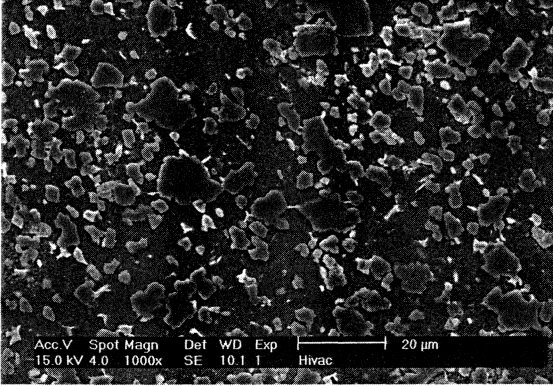


Figure 3 : Scanning electron micrograph of AlSi25Cu4Mg1

Figure 4: Si - particle with twins

In the extrudates, at the interface of the Si-particles dislocations are visible. Their origin is supposed to be the mismatch strain generated both by the different deformation behavior during the extrusion process and the different thermal expansion of the Al-matrix and the Si-particles during cooling after the extrusion. The Al-matrix contains beneath the Si-particles also various smaller precipitates. Among these yet the intermetallic phase Mg_2Si could be identified. Further studies will concentrate on the identification and the quantification of the precipitates and their dependence on the extrusion temperature.

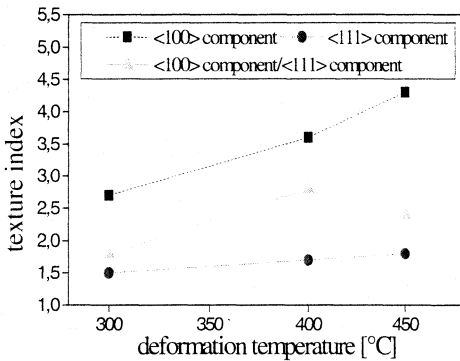


Figure 5 Texture index versus extrusion temperature

5 Texture

Texture analyses were performed at cross sections of the extrudates using X-rays. The Si-particles due to their high strength and shape as well as due to the high density of the billets (before hot extrusion) do not show any preferred orientation. In the center of the samples the aluminum matrix develops a $\langle 111 \rangle$ - $\langle 100 \rangle$ double fiber texture with a very weak $\langle 100 \rangle$ component. With increasing billet temperature the $\langle 100 \rangle$ component increases in strength while the strength of the $\langle 111 \rangle$ fiber component appears to be rather independent of the

deformation temperature (fig. 5). This fiber texture is different to findings of /7/ on single-phase aluminum alloys, which showed a dominant $\langle 111 \rangle$ - fiber. With regard to the temperature dependence of the $\langle 100 \rangle$ fiber, /7/, however, found a similar increase of the increase in strength of the $\langle 100 \rangle$ -fiber with increasing temperature. By further substructure characterization /7/ concluded that this might be due to a higher recovery rate in the $\langle 100 \rangle$ component.

6 Residual Stresses

For residual stress analyses on the surface of the extrudates at 300° C X-rays were used, while the residual stress state in the bulk of the samples was determined non-destructively by a recently developed method using high energy synchrotron radiation /8, 9/. The results of the experiments show (fig. 6) that the residual stress state in axial direction in the bulk of the sample is characterized by low residual macrostresses but high phase specific residual stresses.

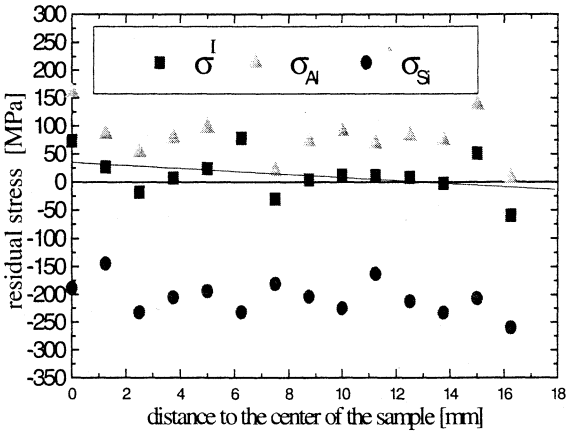


Figure 6: Residual stresses in axial direction in the sample extruded at 450°C

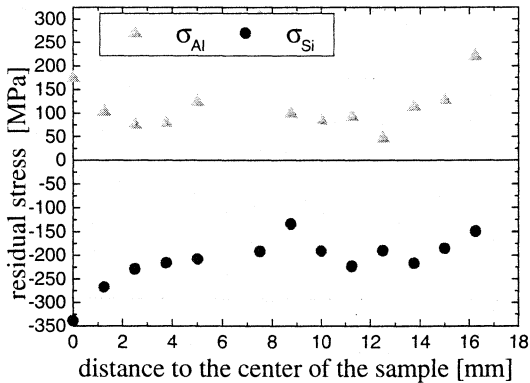


Figure 7 Residual stresses in hoop direction in the sample extruded at 450°C

The macrostress state is typical for the residual stress distribution evolving due to temperature gradients during cooling but it also may result from the chosen extrusion ratio, since former investigations of the residual stresses in cold extruded steel revealed a similar residual stress pattern in case of extrusion ratios larger than $\phi = 1.6$ [10]. Due to the differences in the thermal expansion coefficient the residual stresses in the Al-matrix are tensile stresses of 100 MPa, approximately.

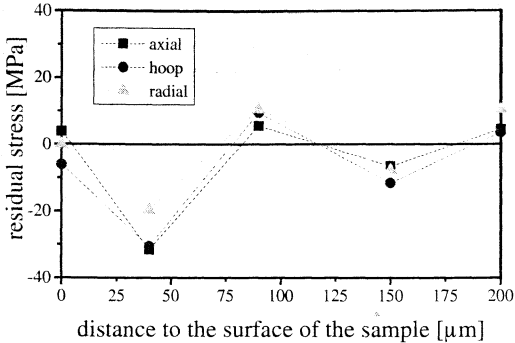


Figure 8: Residual stress in Al-matrix, conditions s. tab.1, 300°C

The Si-particles contain the balancing compressive residual stresses of - 225 MPa approximately. A comparison of the residual stress values obtained in axial direction (fig. 6) and hoop direction (fig. 7) reveals that the residual stress state at all positions investigated across the sample diameter is nearly hydrostatic.

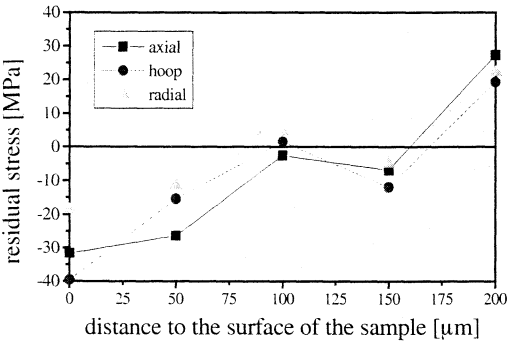


Figure 9: Residual stress in Al-matrix conditions s. tab.1, 400°C

The residual stress distribution near the extrudates pressed at the conditions given in tab.1 at 450°C and 300°C is shown in fig. 8 to fig. 11. Similar to the results of the residual stress analyses in the bulk of the samples also near the surface the residual stresses in both phases are nearly hydrostatic, even within the penetration depth of the X-radiation of 30μm, approximately. In the Si higher compressive stresses than in the Al-matrix, are present, in the Al-matrix even tensile stresses are found in a depth of more than 100μm. The residual stress distribution show a surface effect directly at the surface, but, with increasing depth the residual stress level in both the Al-matrix and the Si-particles approaches the residual stress level determined in the bulk. The residual stress distribution near the surface of the sample

extruded by 300°C and 400°C respectively 450°C do not show significant differences within the error margin of ± 40 MPa.

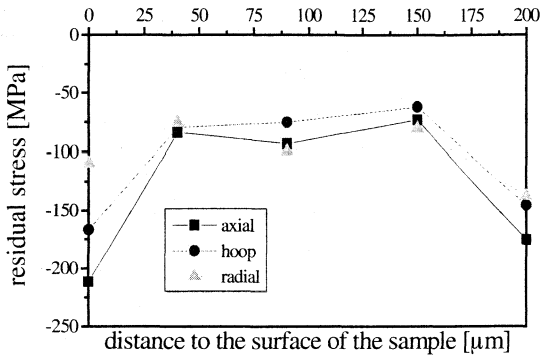


Figure 10: Residual stress in Si-particles, conditions s. tab.1, 300°C

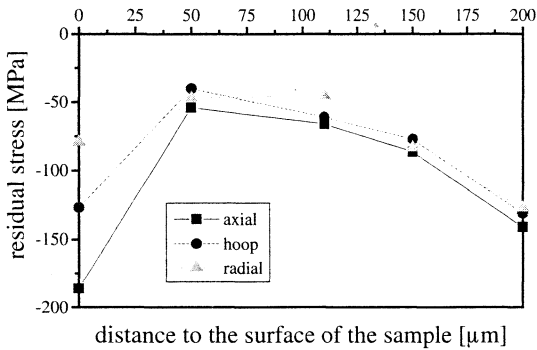


Figure 11: Residual stress in Si-particles, conditions s.tab.1, 450°C

7 Conclusions and Outlook

Analyses of the microstructure, the texture and the residual stresses in hot extruded AlSi25Cu4Mg1 reveal that the appearance of the microstructure in optical and scanning electron micrographs is stable under the extrusion conditions displayed in tab.1 up to an extrusion temperature of 450° C. Future investigations will concentrate on comparing also the precipitates and dislocation arrangement. Texture analyses showed a strong dependence of the strength of the components of the $\langle 111 \rangle$ - $\langle 100 \rangle$ double fiber texture on the extrusion temperature and also hint to a dependence on the extrusion velocity which will be further studied. Additionally, the tensile tests are planned for assessing the influence of the different fiber texture on the formability of the extrusion products. The residual stress state analyses reveal that the residual stresses both in the Al-matrix and the Si particles is nearly hydrostatic. Within the Si-particles the residual stresses are compressive, the Al-matrix contains tensile

residual stresses. There are small compressive macro residual stresses near the surface of the samples.

8 Acknowledgements

The authors are grateful for the support of Mr. Schubert-Bischoff for the sample preparation for TEM investigations and for the allocation of beam time beamtime ID15a at the ESRF Grenoble. The financial support (Mu 864/8-1) by the Deutsche Forschungsgemeinschaft is gratefully acknowledged.

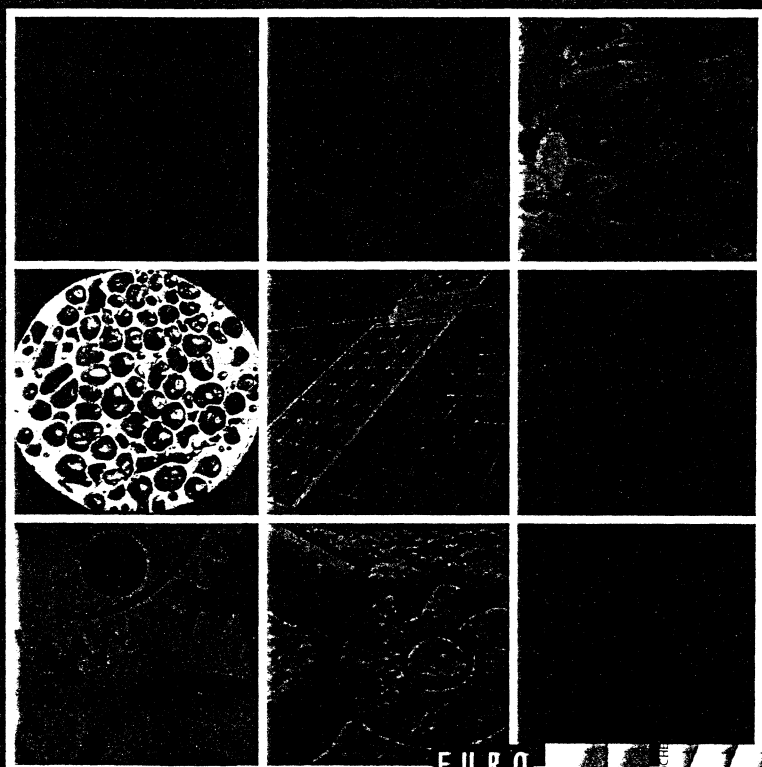
9 References

- /1/ K. Hummert; Moderne Aluminiumlegierungen über Pulvermetallurgie und Sprühkompaktieren für den Einsatz in Verbrennungsmotoren, Sonderdruck PEAK Werkstoffe
- /2/ P. Stocker, F. Rückert, K. Hummert; Die neue Aluminium-Silizium-Zylinderlaufbahn-Technologie für Kurbelgehäuse aus Aluminiumdruckguß, Sonderdruck Motortechnische Zeitschrift 58 (1997), Friedrich Vieweg & Sohn Verlagsges. mbH
- /3/ Forschungszentrum Strangpressen, Technische Universität Berlin, Research and Development in Extrusion, <http://www.fzs.TU-Berlin.De/>
- /4/ K.Müller, Th.Teubert, Proc. ICAA-5, Grenoble,1996, Vol.4, pp. 91-99
- /5/ K.Müller, E. Hellum, Proc. ICAA-6, Toyohashi, 1998, Vol.1, pp. 419-424
- /6/ K.B.Müller, U.Winsemann, Aluminium 75 (1999), 4, pp.314-320, (part 1) and Aluminium 75 (1999), 6, pp. 531-536 (part 2)
- /7/ H.E. Vatne, K.Pedersen, O.Lohne, G. Jenssen, Textures and Microstructures 30 (1997), pp. 81 – 95
- /8/ W. Reimers, A. Pyzalla; M. Broda, G. Brusch, D. Dantz, K.-D. Liss, T. Schmackers, T. Tschentscher, J. Mat. Sci. Letters 19 (1999), pp. 581 - 583
- /9/ A.Pyzalla, W.Reimers, A.Royer, K.-D.Liss, Proc. 20th Risoe International Symposium on Materials Science: Deformation-Induced Microstructures: Analysis and Relation to Properties. Editors: J.B.Bilde-Soerensen et al. Risoe National Laboratory, Roskilde, Denmark (1999), pp. 453 - 458
- /10/ A.Pyzalla, W.Reimers, K.Pöhlandt, Proc. ICRS 5, (T.Ericsson, M.Odén, A.Andersson eds.) 16 - 18. Juni 1997, Linköping, Schweden, pp. 58 - 63

Microstructural Investigation and Analysis

EUROMAT – Volume 4

Edited by B. Jouffrey and J. Svejcar



FMS

EUROMAT

 MATERIALICA
VERSITÄT

DCM